Front. Struct. Civ. Eng. 2020, 14(2): 411–434
https://doi.org/10.1007/s11709-019-0602-y

RESEARCH ARTICLE

Mechanical properties characterization of different types of masonry infill walls

André FURTADO[a], Hugo RODRIGUES[b*], António ARÊDE[a], Humberto VARUM[a]

[a] *CONSTRUCT-LESE, Department of Civil Engineering, Faculty of Engineering, University of Porto, Porto 4200-465, Portugal*

[b] *RISCO, School of Technology and Management, Polytechnic Institute of Leiria, Leiria 2411-901, Portugal*

[*] *Corresponding author. E-mail: hugo.f.rodrigues@ipleiria.pt*

ABSTRACT It is remarkable, the recent advances concerning the development of numerical modeling frameworks to simulate the infill panels' seismic behavior. However, there is a lack of experimental data of their mechanical properties, which are of full importance to calibrate the numerical models. The primary objective of this paper is to present an extensive experimental campaign of mechanical characterization tests of infill masonry walls made with three different types of masonry units: lightweight vertical hollow concrete blocks and hollow clay bricks. Four different types of experimental tests were carried out, namely: compression strength tests, diagonal tensile strength tests, and flexural strength tests parallel and perpendicular to the horizontal bed joints. A total amount of 80 tests were carried out and are reported in the present paper. The second objective of this study was to compare the mechanical properties of as-built and existing infill walls. The results presented and discussed herein, will be in terms of strain-stress curves and damages observed within the tests. It was observed a fragile behavior in the panels made with hollow clay horizontal bricks, without propagation of cracks. The plaster increased the flexural strength by 57%.

KEYWORDS masonry infill walls, experimental characterization, compression strength, shear diagonal strength, flexural strength

1 Introduction

The masonry infill walls are widely used for partition purposes and to provide thermal and acoustic insulation to the reinforced concrete structures. Many of the different types of masonry units developed throughout the last decades to optimize those characteristics and/or to use innovative and green materials (see Figs. 1 and 2). The recent codes' demands regarding the thermal and acoustic insulation of buildings also motivated the development of new materials and new construction techniques of the buildings' facades. The construction methodology to build the buildings' facades modified slightly over the years. Started with the use of one single infill panels made with hollow clay horizontal brick (HCHB) units, which were later replaced using double-leaf, walls (both composed by HCHB units with different thicknesses). More recently, single leaf infill panels made with units with special thermal and acoustic properties are commonly used or, on the other hand, panels made with HCHB units combined with the application of an external thermal insulation composite system has become very popular.

On one hand, the codes focus and requirements of these functional characteristics are increasing, and the continuous increment of the demands to maximize the comfort of the buildings' users is notorious. On the other hand, the contribution of the masonry infill walls to the structural response of reinforced concrete buildings when subjected to an earthquake continues to be ignored and disregarded by some structural codes.

It is remarkable, the advances observed during the last decade in terms of development of numerical modeling frameworks resorting to strut models' concepts or detailing modeling approaches capable of simulate the infill panels' seismic behavior with good accuracy [1,2]. The development of the strut models' concept was originally to capacitate the numerical analyses of infilled frames with higher shear stiffness. Multi-strut models were developed

Article history: Received Dec 6, 2018; Accepted Apr 4, 2019

to simulate the shear behavior and tensile stresses within the contact length between wall and frame.

Numerical models have started to become more and more complex, with some them considering the infills' stiffness and strength degradation under dynamic loads, or other equivalent approaches to simulate the shear sliding failure. Recently, some developments regarding the strut models that are capable to simulate the combined in-plane (IP) and out-of-plane (OOP) behavior have emerged [3–6]. The major advantage of the strut modeling approach is their simplicity of implementation for the analysis of an entire building structure, the capability of simulating the global response of the panels and the corresponding influence on the structural response. The capacity of simulating the global response of the panels and the corresponding influence on the structural response is obviously an important advantage since it requires lower computational effort.

However, there is a lack of experimental data concerning their mechanical and material properties to use and calibrate the numerical models. Additional experimental data about material and mechanical properties of masonry infill walls made with different types of material are needed to provide useful information to the structural designer which will use to obtain accurate numerical models. Few experimental campaigns are available in the literature concerning the characterization of the infill masonry walls mechanical properties [7–10]. However, it is still reduced the amount of information due to the large variability of materials used in the construction and in particular in which concerns to the infill panels made with HCHB units.

In the present paper an extensive experimental campaign comprised a set of mechanical characterization tests on masonry infill walls made with three different types of masonry units: lightweight thermo-acoustic concrete blocks with vertical hollows (VHCB) and HCHB with two different thicknesses.

Specimens with and without plaster were built under laboratory conditions. Additionally, small panels (without visible damage) were collected from existent infill walls in the laboratory to compare the results with the corresponding as-built ones. Four different types of experimental tests were carried, namely: compressive strength tests according to EN1052-1 [11], diagonal tensile strength tests according to ASTM E 519-02 [12] and RILEM TC 76-LUM [13], and flexural strength tests parallel and perpendicular to the horizontal bed joints according to EN 1052-2 [14]. A total amount of 80 tests were carried out. Details regarding the specimens' geometric dimensions, material properties, test setup and instrumentation will be described for each type of test. The results presented and discussed herein, will be in terms of strain-stress curves and damages observed within the tests. Lastly, the following issues will also be studied: the differences between the responses of the specimens made with concrete blocks or clay bricks, the influence of plaster, and the difference between the existing and the as-built specimens.

2 Description of masonry infill units and walls used for experimental testing

The primary objective of this section is to present the experimental campaign that was carried out. The tests were performed in specimens made with three different types of masonry units, namely:

Infill wallet type 1: Panel built with HCHB units. For this study, HCHB unites with two different thicknesses were adopted: 110 and 150 mm, respectively, HCHB110 and HCHB150.

These types of bricks are one of the most common masonry units in Portugal and in the Southern European countries, which are quite used, for example, to build double-leaf walls where the external leaf is typically composed by HCHB110 units and the internal one by the HCHB150 units. Figure 1 shows two examples of RC buildings where it was used HCHB masonry units for the buildings' facades. The geometric dimensions of each

(a) (b)

Fig. 1 Examples of buildings built with HCHB: (a) residential and commercial 5-storey building in Portugal (Portugal); (b) residential 17-storey building in Coruna (Spain).

masonry units can be found in Figs. 3(a) and 3(b), respectively.

Infill wallet type 2: Panel built with VHCB, which consists in a lightweight concrete block with advanced acoustic and thermal. This type of masonry unit started becoming quite common after 1990 in the buildings' facades in Portugal. This type of block is nowadays designed for single leaf facade' walls or in contact with unheated areas. It can also be used in partitions between fire-stairs, stairwells, and elevators. Presently, it constitutes an alternative solution to the double-leaf solutions with light insulation in the intermediate air box and to the simple wall solutions with light insulation in the outside surface (ETICS). Due to this, this masonry unit presents an interesting breathing capacity, which avoids undesirable condensations inside the dwellings. Figure 2 presents two examples of RC buildings built with VHCB315 units. As can be observed in Fig. 3(c), the block consists of 11 longitudinal partitions separated by ten micro-air boxes, which together with the lightweight autoclaved aerated concrete, can reduce the thermal transmission coefficients.

Infill wallet type 3: panels that were collected from existing infill walls in laboratory (herein designated as "existent" wallets), which were made with HCHB150 units, with or without plaster. Vertical and horizontal cuts were performed by technical staff specialized in demolitions. After normalized the dimensions of the specimen, it was included a top layer of mortar to regularize the top and bottom parts of the specimens.

Concerning the material properties of each type of masonry unit, Table 1 provides the main characteristics that can be found in the datasheet provided by the manufacturer. From the datasheet content, it is important to highlight the fact that none of the manufacturers provided information regarding a specific value for the masonry units' compressive strength. According to the manufacturers' estimation the VHCB315 units' compressive strength is around 2.15 times higher than the clay brick units' ones.

Relatively to the thermal transmission coefficient (U), the HCHB110 and HCHB150 units have nominal values equal to 0.29 and 0.42 m^2K/W, which are 45% and 20% lower than that of the VHCB315 unit. Lower differences are noticed regarding the acoustic insulation where differences are around 25% and 20%, respectively (the HCHB110 and HCHB150 results are lower).

No plaster was used for the specimens that were built in laboratory with VHCB315 and HCHB110. Regarding the specimens made with HCHB150 units, 11 of them were built with 10 mm plaster (only in one face of the specimen). The specimens with plaster, herein designated HCHB150P10, were tested to assess the flexural strength

(a) (b)

Fig. 2 Examples of buildings built with VHCB315: (a) residential and commercial 4-storey building in Soure (Portugal); (b) residential 8-storey building in Lisboa (Portugal).

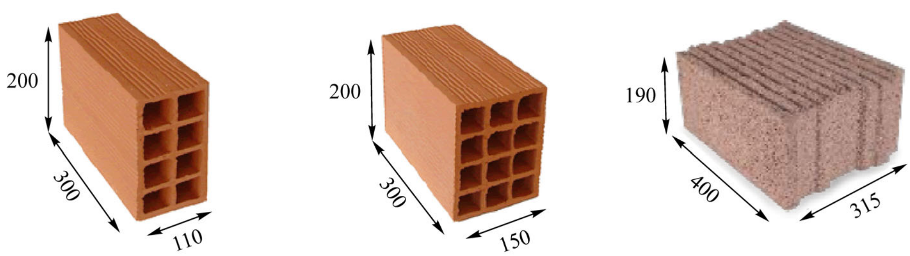

(a) (b) (c)

Fig. 3 Masonry units used in the experimental campaign: (a) HCHB110; (b) HCHB150; (c) VHCB315.

Table 1 Summary of the masonry units' material properties (information provided by the product datasheet)

material properties	HCHB110	HCHB150	VHCB315
compressive strength $f_{c,unit}$ (MPa)	⩾1.5	⩾1.5	⩾3.25
content of active soluble salts	S0 category	S0 category	S0 category
fire reaction	A1 Euroclass	A1 Euroclass	A1 Euroclass
masonry unit mass (kg/unit)	3.9	5.2	20
thermal transmission coefficient U (m^2K/W)	0.29	0.42	0.51
acoustic insulation R_w (dB)	40	43	53
voids (%)	57.7	57.9	26.9

and to compare the results with and without plaster.

The construction methodology adopted to build the specimens with HCHB units was according to the current practice adopted in the southern European countries. Vertical and horizontal bed joints with approximately 10 mm thickness were assumed. Concerning the infill panels made with VHCB315 masonry units, it was assumed the construction procedure recommended by the manufacturer was very common for this type of masonry unit. The procedure is characterized by full bedded horizontal joint (10 mm thick) and a partial vertical bed joint (only the central interlock hole was filled with mortar), as can be observed in Fig. 4. This construction procedure is required by the manufacturer to ensure that all the dozens of air chamber are empty to achieve lower coefficients of thermal transmission and high ventilation capacity.

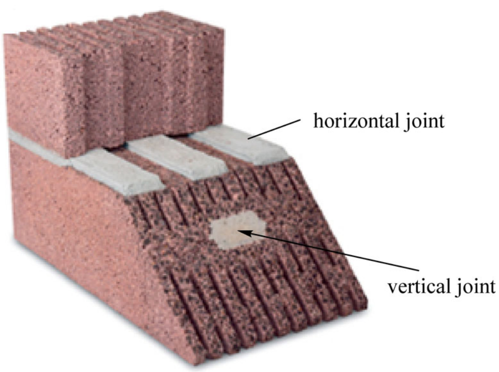

Fig. 4 Infill panels made with VHCB315 masonry units: construction methodology.

The wall specimens were made using an industrial ready-mix mortar with a M5 class. Samples of the mortar used in the specimens' construction were collected in order to assess the compressive and tensile strength according to the standard EN 1015-11 [15]. The results from the mortar testing are summarized in Table 2 according to each specimens' group and the respective type of experimental test that will be subjected to. Slight variations can be found due to workmanship and to the variability and high sensibility of the materials to the water contents of the mortar. Mortar samples were grouped according to the type of tests made on the infill panels which they were used in, namely:

Group A — Compressive strength tests;

Group B — Diagonal tensile strength tests;

Group C — Flexural strength tests parallel to the horizontal bed joints;

Group D — Flexural strength tests perpendicular to the horizontal bed joints.

3 Experimental campaign

Four different types of tests were carried out, namely compressive strength tests using 3 specimens, the number minimum according to EN1052-1 [11], diagonal tensile strength tests also in 3 specimens, (the minimum according to ASTM E 519-02 [12]), flexural strength tests parallel and perpendicular to the horizontal bed joints (for which the number minimum of specimens according to EN 1052-2 [14] is 5 of each type). Each type of test and the corresponding number of specimens tested are summarized in Table 3.

4 Compressive strength tests

Compressive strength tests were carried out in order to achieve the compressive strength and the elastic modulus perpendicular to the horizontal bed joints according to the standard EN 1052-1 [11]. The test consists in the application of a distributed vertical compressive loading in the top surface of the specimen until reaching failure. For this, a servo-hydraulic actuator with a maximum capacity of 1500 kN (±75 mm) for the specimens made with VHCB315 units (Fig. 5(a)) and a servo-hydraulic actuator with a maximum capacity of 100 kN (±100 mm) for the specimens made with HCHB units (Fig. 5(b)) were used. Concerning to the remaining test setup, it was used a steel profile attached to the actuator was used to distribute

Table 2 Summary of the mortar material properties of each specimens' group

type of tested masonry infill panels	A		B		C		D	
	$f_{c,m}$ (MPa)	$f_{t,m}$ (MPa)	$f_{c,m}$ (MPa)	$f_{t,m}$ (MPa)	$f_{c,m}$ (MPa)	$f_{t,m}$ (MPa)	$f_{c,m}$ (MPa)	$f_{t,m}$ (MPa)
VHCB315	6.10	2.03	6.52	2.18	4.83	1.59	4.74	1.80
HCHB110	8.08	2.75	8.08	2.75	10.61	3.28	8.08	2.75
HCHB150	13.35	4.51	12.38	4.76	14.13	4.98	14.13	4.98
HCHB150P10	N/A	N/A	N/A	N/A	12.95	4.52	12.95	4.52
HCHB150 (existent)	11.90	9.03	11.90	9.03	11.90	9.03	11.90	9.03
HCHB150P10 (existent)	12.60	5.18	N/A	N/A	12.60	5.18	N/A	N/A

Note: N/A: Not applicable.

Table 3 Summary of the experimental campaign: number of specimens tested

type of masonry infill panels	compressive strength tests	diagonal tensile strength tests	flexural strength tests parallel to the horizontal bed joints	flexural strength tests perpendicular to the horizontal bed joints
VHCB315	3	3	5	5
HCHB110	5	4	5	5
HCHB150	5	5	5	5
HCHB150P10	N/A	N/A	6	5
HCHB150 (existing)	4	1	1	3
HCHB150P10 (existing)	4	N/A	1	N/A
total	21	13	23	23

Note: VHCB315: panels made with VHCB with 315 mm thickness and no plaster; HCHB110: panels made with HCHB with 110 mm thickness and no plaster; HCHB150: panels made with HCHB with 110 mm thickness and no plaster; HCHB150P10: panels made with HCHB with 150 mm thickness with 10 mm plaster; HCHB150 (existent): panels made with HCHB with 110 mm thickness and no plaster taken from existing full-scale wall panels in Laboratory; HCHB150P10 (existent): panels made with HCHB with 110 mm thickness, with 10 mm plaster, taken from existing full-scale wall panels in laboratory.

(a) (b)

Fig. 5 Compressive strength tests: (a) test setup specimens made with VHCB315 masonry units; (b) specimens made with HCHB masonry units.

the vertical loading throughout the specimen top surface. A hinged connection between the hydraulic actuator and the steel profile was used to accommodate possible irregularities or eccentricities.

The specimens' geometric dimensions were defined according to the standard EN 1052-1 [11] recommendations which are summarized in Table 4, and shown in Fig. 6, where l_u and h_u are the masonry unit length and height, respectively. Lastly, l_s, h_s, and t_s are the masonry wallets length, height and thick.

The VHCB315 specimens' dimensions were defined to be 800 mm ×1000 mm, wide and high, respectively (Fig. 7(a)). Regarding the remaining specimens made with HCHB units, all of them were defined to be 600 mm × 600 mm, wide and high, respectively (Fig. 7(b)).

The instrumentation was assumed according to the standard EN 1052-1 [11], which consists in two pairs of vertical linear variable differential transformer (LVDT) transducers in each specimen face and one horizontal transducer in each face of the specimens. The disposition of the instrumentation used for each specimen group is presented in Fig. 7.

4.1 Experimental results

The compressive strength (f_c) of each specimen was calculated according to EN 1052-1 [11] procedure namely, using the maximum force applied until failure occurs. The force was divided by the area in which it was applied the compression loading. From a set of experiments the characteristic compressive strength ($f_{c,k}$) can be assumed as the lower value of two conditions: $f_{c,mean}/1.2$ (where the $f_{c,mean}$ stands for the mean compressive strength of a set of

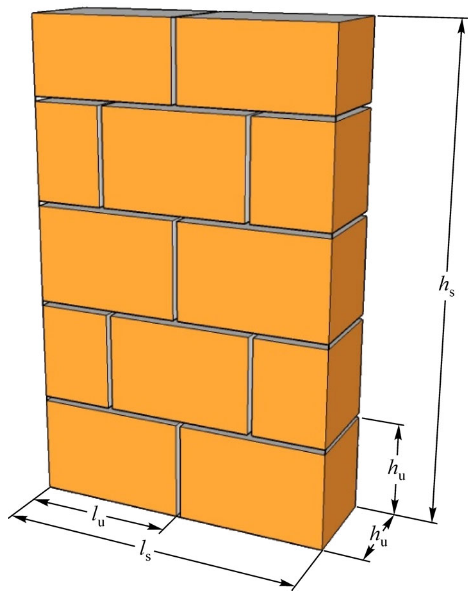

Fig. 6 Compressive strength tests: specimens' geometric dimensions according to standard EN 1052-1 [11] recommendations.

Table 4 Masonry infill panels geometric dimensions according to the standard EN 1052-1 [11] recommendations

masonry unit dimensions		masonry infill panels' geometric dimensions			
l_u (mm)	h_u (mm)	length l_s (mm)	height h_s (mm)		thickness t_s (mm)
⩽300	⩽150	⩾(2×l_u)	⩾5 h_u	⩾3 t_s and⩽15t_s and⩾t_s	⩾t_u
	>150		⩾3 h_u		
>300	⩽150	⩾(1.5×l_u)	⩾5 h_u		
	>150		⩾3 h_u		

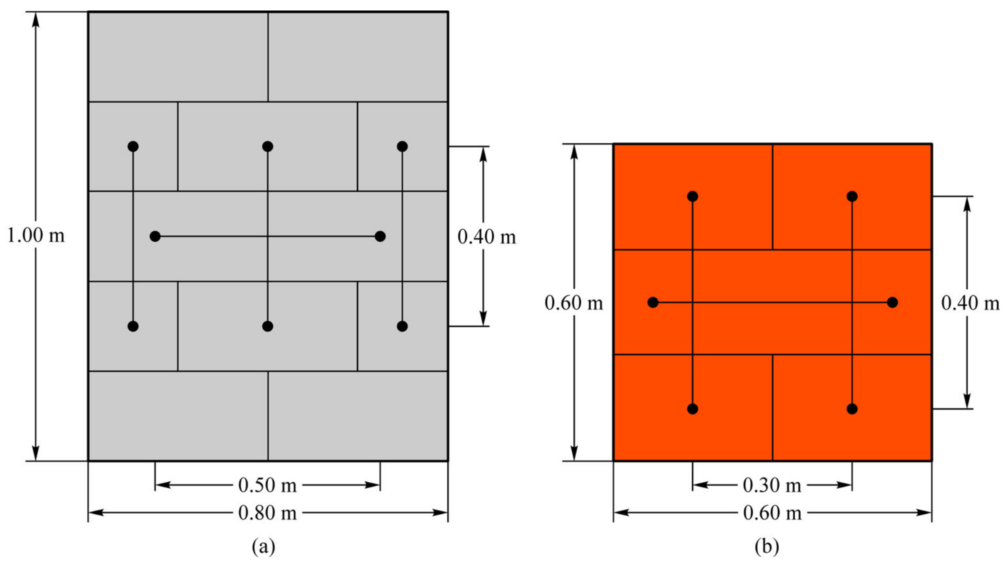

Fig. 7 Compressive strength tests: specimens' geometric dimensions and instrumentation: (a) VHCB315; (b) HCHB specimens.

experiments; $f_{i,min}$ which is the minimum compressive strength obtained by a specimen in a set of experiments. For each specimen it was also calculated the elastic modulus (E) according to the EN 1052-1 [11] which consists in the secant elasticity modulus for a stress equal to 1/3 of the maximum one and the corresponding average strain taken from all vertical LVDTs measurements. The stress-strain curves obtained for each group of specimens are plotted in Fig. 8. The following parameters were determined for each group: mean, standard deviation (SD),

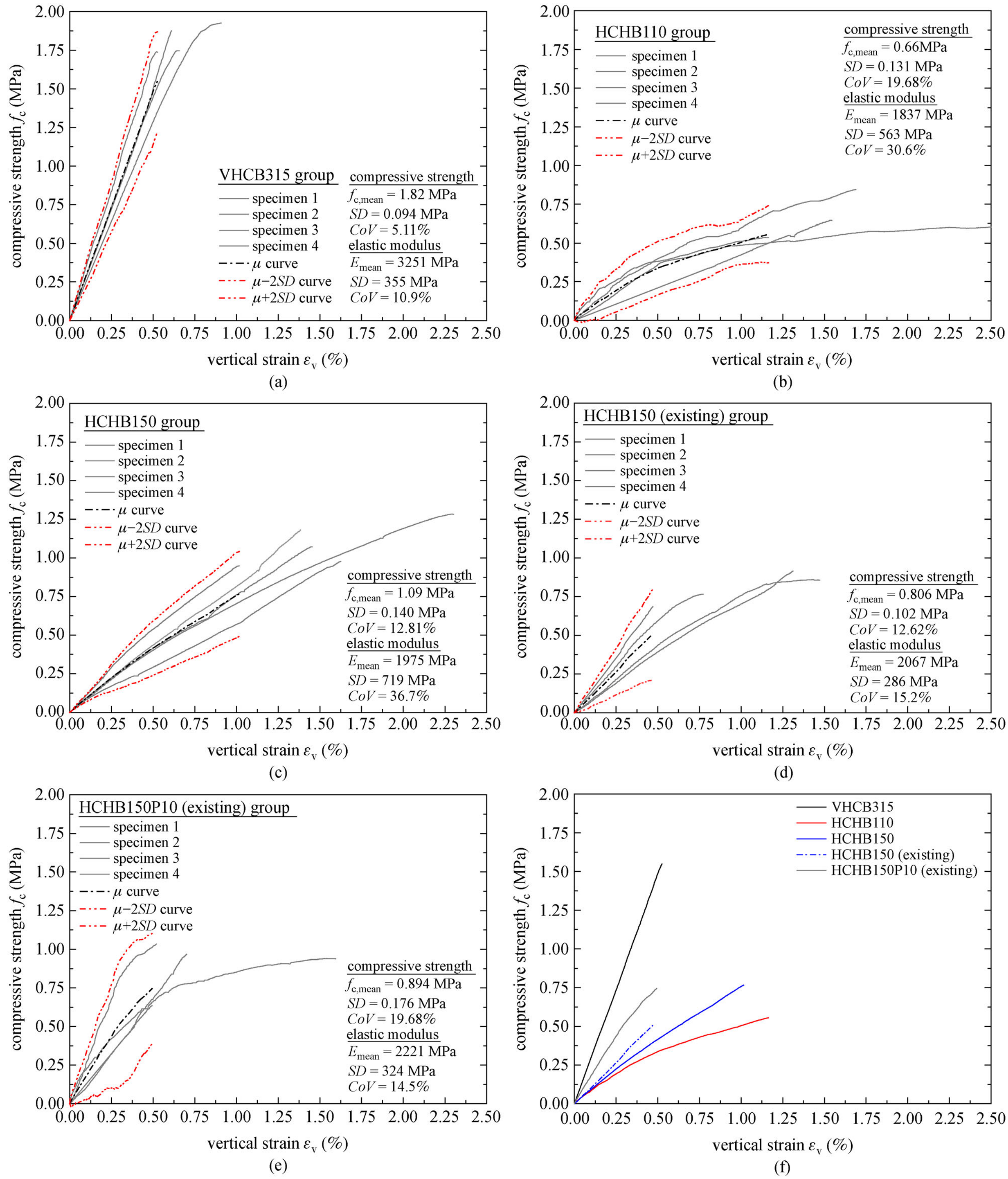

Fig. 8 Compressive strength test results: Stress vs Strain curves: (a) VHCB315; (b) HCHB110, (c) HCHB150 and (d) HCHB150 (existent); (e) HCHB 150P10 (existent); (f) global average curves.

and coefficient of variation values (*CoV*). From the strain-stress curves, the following observations can be drawn:

1) The VHCB315 group achieved the highest mean compressive strength equal to 1.82 MPa and the lowest *CoV* equal to 5.11%. The lowest compressive strength was reached by the HCHB110 group with 0.66 MPa.

2) By comparing the results between the HCHB110 and the HCHB150, it can be observed that the last one achieved the mean compressive strength equal to 1.09 MPa, which is 40% higher than the result obtained by the HCHB110 group. On the other hand, larger variability was found in the HCHB110 specimens' tests.

3) From the comparison between the groups HCHB1510 and HCHB150 (existing), it can be observed that the last group reached a mean compressive strength equal to 0.806 MPa, 18% lower than the HCHB150 but with similar *CoV*. Besides the material properties variability, no specific reason can justify this difference since the mortar compressive strength of the HCHB150 specimens is slightly higher than that used in HCHB150 (existing) specimens. Some minor cracking induced by the preparation of the HCHB150 (existing) specimens may affected the results.

4) The HCHB150P10 (existing) specimen reached a mean compressive strength of 0.894 MPa, which is 10% higher when compared with the results of the HCHB150 (existing) group results.

Finally, Fig. 8(e) includes the plots of the average curves obtained from each group tests in which some differences among them can be detected. For example, for a vertical strain of 0.25% the VHCB315 reached a mean compressive strength of 0.77 MPa, 40% higher than the HCHB150P10 group, 66% higher than the HCHB150 (existent), 69% higher than the HCHB150 group and, finally, 71% higher than the HCHB110 specimens' group. Larger differences were found for larger vertical strain values.

Table 5 provides a summary of the compressive strength statistical parameters obtained by each group of specimens.

The statistical parameters obtained for the specimens' elastic modulus are summarized in Table 6. From those results, it was found again that the VHCB315 group achieved the highest result with 3251 MPa. The HCHB110 group with a mean elastic modulus equal to 1837 MPa achieved the lowest result. On the other hand, slight differences can be observed between the groups HCHB150 and HCHB150 (existing), which can be justified by the presence of mortar inside of some of the brick perforations in the case of the HCHB150 (existing) group. By comparing the results from the existing specimens with and without plaster, it can be found that the plaster contributed to the increase around 7%.

Additionally, it was computed the ratio between the infill panels' compressive strength and the corresponding elastic modulus. From the results, it can be found that the highest value was achieved by the HCHB110 group and the lowest one by the VHCB315 group with a ratio equal to 2783 and 1786, respectively. The results obtained by the HCHB150 group is 35% lower than that of obtained by the group HCHB110. From the comparison between the ratios obtained by the groups HCHB150 and HCHB150 (existent), it can be observed that the existent one is 30% higher, which can be related to the combination of lower compressive strength and higher elastic modulus. Concerning only to the existing specimens, it seems that the plaster did not contributed to higher $E_{mean}/f_{c,mean}$ ratio.

Looking for some results available in the literature, it can be found that Pereira et al. [16] carried out compressive strength tests in small infill panels made with HCHB150 units from which obtained a mean compressive strength equal to 1.26 MPa (13% higher), an elastic modulus equal to 1577 MPa (13% lower) and a ratio $E_{mean}/f_{c,mean}$ equal to 1252. This result is 31% lower than the one obtained by the HCHB150 group within this testing campaign.

Through the literature, it is possible to find some analytical relationships between the infill panels' com-

Table 5 Compressive strength results: statistical parameters

statistical parameter	VHCB315	HCHB110	HCHB150	HCHB150 (existing)	HCHB150P10 (existing)
$f_{c,mean}$ (MPa)	1.82	0.66	1.09	0.806	0.894
SD (MPa)	0.094	0.131	0.140	0.102	0.176
CoV (%)	5.11	19.68	12.81	12.62	19.68
$f_{c,k}$ (MPa)	1.52	0.54	0.91	N/A	N/A

Note: N/A: Not applicable.

Table 6 Elasticity modulus results: statistical parameters

statistical parameter	VHCB315	HCHB110	HCHB150	HCHB150 (existing)	HCHB150P10 (existing)
E_{mean} (MPa)	3251	1837	1975	2067	2221
SD (MPa)	355	563	719	286	324
CoV (%)	10.9	30.6	36.7	15.2	14.5
$E_{mean}/f_{c,mean}$	1786	2783	1811	2564	2484

pressive strength and their elastic modulus that were proposed by different authors. In 1971, Sahlin [17] proposed the relationship expressed by the Eq. (1):

$$E_{\mathrm{m}} = 750 f_{\mathrm{m}}. \tag{1}$$

While Sinha and Pedreschi [18] proposed Eq. (2):

$$E_{\mathrm{m}} = 1180 f_{\mathrm{m}}^{0.83}. \tag{2}$$

Later, Bartolomé [19] proposed Eq. (3):

$$E_{\mathrm{m}} = 500 f_{\mathrm{m}}. \tag{3}$$

Hendry [20] reported Eq. (4):

$$E_{\mathrm{m}} = 2116 f_{\mathrm{m}}^{0.50}. \tag{4}$$

Due to the dispersion of values obtained from the analytical prediction, Paulay and Priestley [21] and Sahlin [17] converged in the same expression (Eq. (5)) which is also suggested by Eurocode 6 [22] in Section 3.8.3:

$$E_{\mathrm{m}} = 1000 f_{\mathrm{m}}. \tag{5}$$

By comparing the prediction results according to Eurocode proposal, large differences can be found. The results of the groups HCHB110 and HCHB150 groups are 2.8 and 1.7 times higher than that of the analytical prediction results. This result allow to conclude that this expression must be revised and adapted for infill panels made with different types of masonry units. New empirical analytical predictions were derived based on the experimental results obtained within this experimental campaign for VHCB315, HCHB110 and HCHB150 infill panels and are expressed in Eqs. (6), (7), and (8), respectively. The coefficient of variation of Eqs. (6), (7), and (8) are 9.1%, 38%, and 43%, respectively.

$$E_{\mathrm{m}} = 1786 f_{\mathrm{m}}. \tag{6}$$

$$E_{\mathrm{m}} = 2783 f_{\mathrm{m}}. \tag{7}$$

$$E_{\mathrm{m}} = 1811 f_{\mathrm{m}}. \tag{8}$$

4.2 Damages observed

From the specimens' damages throughout the tests, a remarkable difference can be addressed between the specimens made with horizontal clay bricks and concrete blocks (Fig. 9). The difference consisted in the fragile brittle behavior evidenced by the first ones, with suddenly rupture of the specimens, partial collapse of bricks, without prior visible cracks propagation. On the other hand, the typical damages observed on the VHCB315 specimens are characterized by vertical cracks from the top to the bottom of the specimen (Fig. 9(a)).

The HCHB110 specimens' failure were characterized by the crushing of the first or last row of bricks which lead to the instability of the panel. Similar failures were observed in the remaining groups of HCHB specimens. Finally, it must be considered that the compressive strength tests of the HCHB specimens were sensitive to the existence of prior slight damages in the bricks (slight cracks due to manufactory production or transport).

5 Diagonal tensile strength tests

5.1 Introduction

Diagonal tensile strength tests were carried out according to the American standard ASTM E 519-02 [12] and RILEM TC 76 [13]. This test consists in the application of a diagonal compressive force through two steel loading shoes that are attached to the top and bottom part of a specimen rotated 45× relative to the vertical direction. The top shoe is attached also to a servo-hydraulic actuator with 1500 kN capacity (× 75 mm) allowing to apply a continuous loading until the specimen reaches the rupture (Fig. 9(a)).

Both standards requirements are unanimous, in which concerns to the geometric dimensions of the specimens (independent of the masonry unit thickness): 1200 mm ×1200 mm width and height, respectively (Fig. 10(b)). The minimum number of specimens required is 3. A total amount of 8 transducers were used to monitor the displacements. Obviously, it was assumed the instrumentation recommended by the standard ASTM E 519-02 [12], was to measure of the vertical shortening (ε_{v}) that was captured by a pair of LVDT's (one in each specimen' face) and of the horizontal extension (ε_{h}) by three pairs of LVDT's in each specimen' face (Fig. 10(b)).

The measurement length between the transducers measurement used to calculate the shear straining (Y) was 1000 mm, as recommended by the standard. Additionally, two pairs of horizontal transducers were placed in both specimens' faces with 600 mm length. A total amount of 13 tests were performed in this set of tests, three of them related to VHCB315, four of them to HCHB110, five of HCHB150 and one HCHB150 (existing).

5.2 Experimental results

The shear stress (S_{s}) was computed for each specimen according to Eq. (9), provided by standard ASTM E 519-02 [12], which consists in the relationship between the maximum applied force (P) and the cross-section transverse net area. The shear-stress curves of each specimen versus the vertical shortening and the horizontal extension are plotted in Fig. 10. Additionally, the transverse or shear stiffness (modulus of rigidity), G, of each specimen was

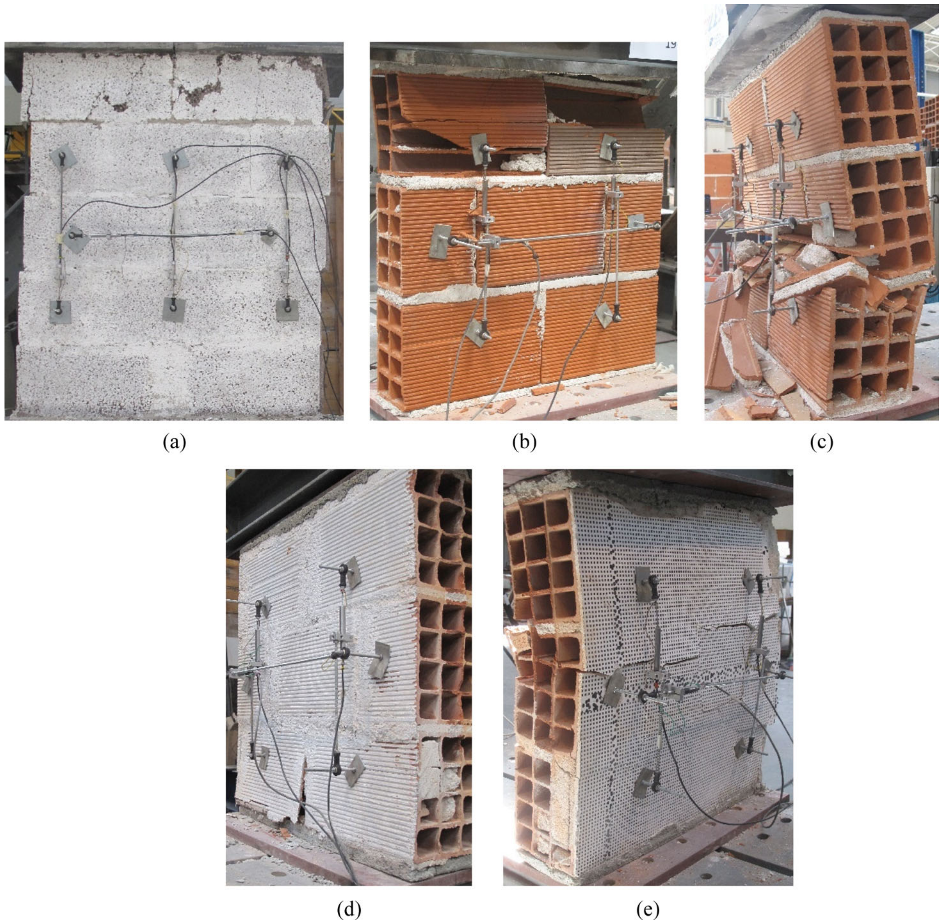

Fig. 9 Compressive strength tests: damages observed: (a) VHCB315; (b) HCHB110, (c) HCHB150; (d) HCHB150 (existent); (e) HCHB150P10 (existent).

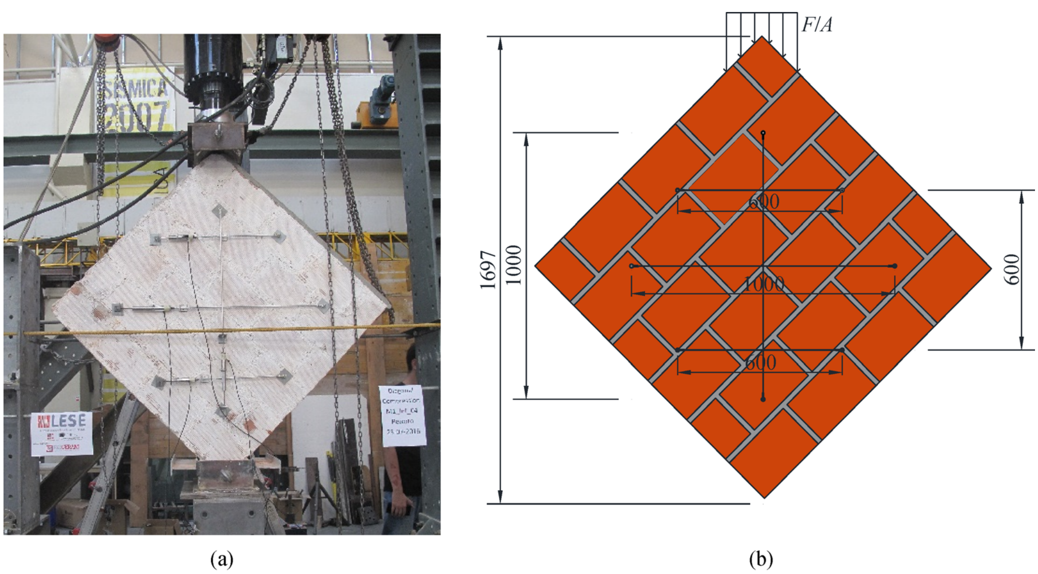

Fig. 10 Diagonal shear tension strength tests: (a) test setup view; (b) instrumentation and geometric dimensions (mm).

calculated based on the shear stress versus shear straining (Y) curves as suggested by the standard. The shear stress results obtained by all the groups are summarized in Table 7.

$$S_{\mathrm{s}} = \frac{0.707 \times P}{A_{\mathrm{n}}}, \tag{9}$$

where S_{s} is the shear stress, P is the maximum applied load, and A_{n} is cross-section transverse net area of the specimen.

From the shear stress-strain curves (Fig. 11) the following observations can be drawn:

1) HCHB 150 group (Fig. 11(c)) achieved the highest shear stresses with mean value of 0.645 MPa, while the lowest one was reached by the VHCB315 group with 0.204 MPa (Fig. 11(a)), which 69% lower.

2) The larger variability among the specimens' results was gathered by the HCHB110 group with *CoV* equal to 35.2% and the lower one again by the VHCB315 group with *CoV* equal to 5.7%.

3) From the comparison between the HCHB110 and HCHB150 it can be detected that the first ones achieved a mean shear stress of 0.565, 13% lower than the second group (Figs. 11(b) and 11(c)).

In Fig. 11(d) it is plotted the shear stress-strain curve for the solo specimen of the HCHB150 (existing) group, that reached a shear stress of 0.38 MPa, thus 49% lower than the result obtained by the HCHB150 group. This can be justified by some slight damages caused by the panel removal which increased some vulnerability to the panel. Table 7 summarizes the shear stress statistical parameters obtained for each group.

From the shear stress-shear strain (Y) curves plotted in Fig. 12, it was found that the highest shear stiffness was obtained by the VHCB315 group (Fig. 12(a)) with a mean value equal to 1389 MPa which is 29% lower than the HCHB150 result (Fig. 12(c)). The HCHB150 group with a mean value equal to 996 MPa reached the lowest shear stiffness. The mean shear stiffness equal to 1141 MPa obtained by the group HCHB110 (Fig. 12(b)) is 13% higher than the group HCHB150. Finally, the shear stiffness obtained by the specimens HCHB150 (existing), shown in Fig. 12(d), was 17% higher than the as-built group.

In Fig. 12(e), the comparison between the global average curves obtained for each group is plotted. Table 8 summarizes the transverse shear stiffness modulus' statistical parameters of each group.

5.3 Damages observed

From the tests' observation, the representative failure modes of each group are presented in Fig. 13. All of them were characterized by the separation between the brick joint interfaces. Some minor cracking was detected in the top and bottom part of the specimens and no pure vertical cracking was observed.

Regarding the specimens made with VHCB315 units, visible progression of cracking during the test was observed. Finally, it occurred sliding failure of two of the HCHB110 specimens (Fig. 13(c)).

6 Flexural strength tests

6.1 Parallel to the horizontal bed joints

6.1.1 Introduction

The flexural strength tests parallel to the horizontal bed joints were carried out according to the EN1052-2 standard (CEN 1999). This type of tests aims at obtaining the masonry infill panels' flexural strength according to the principal direction where the internal forces (bending moments and shear) develop. A servo-hydraulic actuator with a maximum capacity of 100 kN (× 100 mm) was used. The loading was distributed along two linear alignments distanced 330 mm apart for the VHCB315 specimens and 300 mm for the panels made with HCHB units. The loading was applied through two rollers placed between the specimen and the steel profiles attached to the actuator. The rollers are free to rotate, thus allowing the rotation of specimen. The specimen reacted against a steel structure composed also by two horizontal rollers inserted in the steel profiles, as can be observed in Fig. 14. The position of the out-of-plane restrains was defined according to the standard, namely 50 mm distanced from the top and bottom of all the specimens.

The standard NP EN1052-2 standard (CEN 1999) requires some specific rules for the definition of the specimens' dimensions (Fig. 15), namely:

1) Specimens' width: $b \geqslant 400$ mm and $b \geqslant 1.5 l_{\mathrm{u}}$, where l_{u} is the masonry unit length.

2) At least two horizontal joints must be built along the l_2 dimension.

The specimens' geometric dimensions were defined

Table 7 Shear stress statistical results: statistical parameters

statistical parameter	VHCB315	HCHB110	HCHB150	HCHB150 (existent)
$S_{\mathrm{s,mean}}$ (MPa)	0.204	0.565	0.645	0.38
SD (MPa)	0.012	0.199	0.143	N/A
CoV (%)	5.71	35.2	22.2	N/A

Note: N/A: Not applicable.

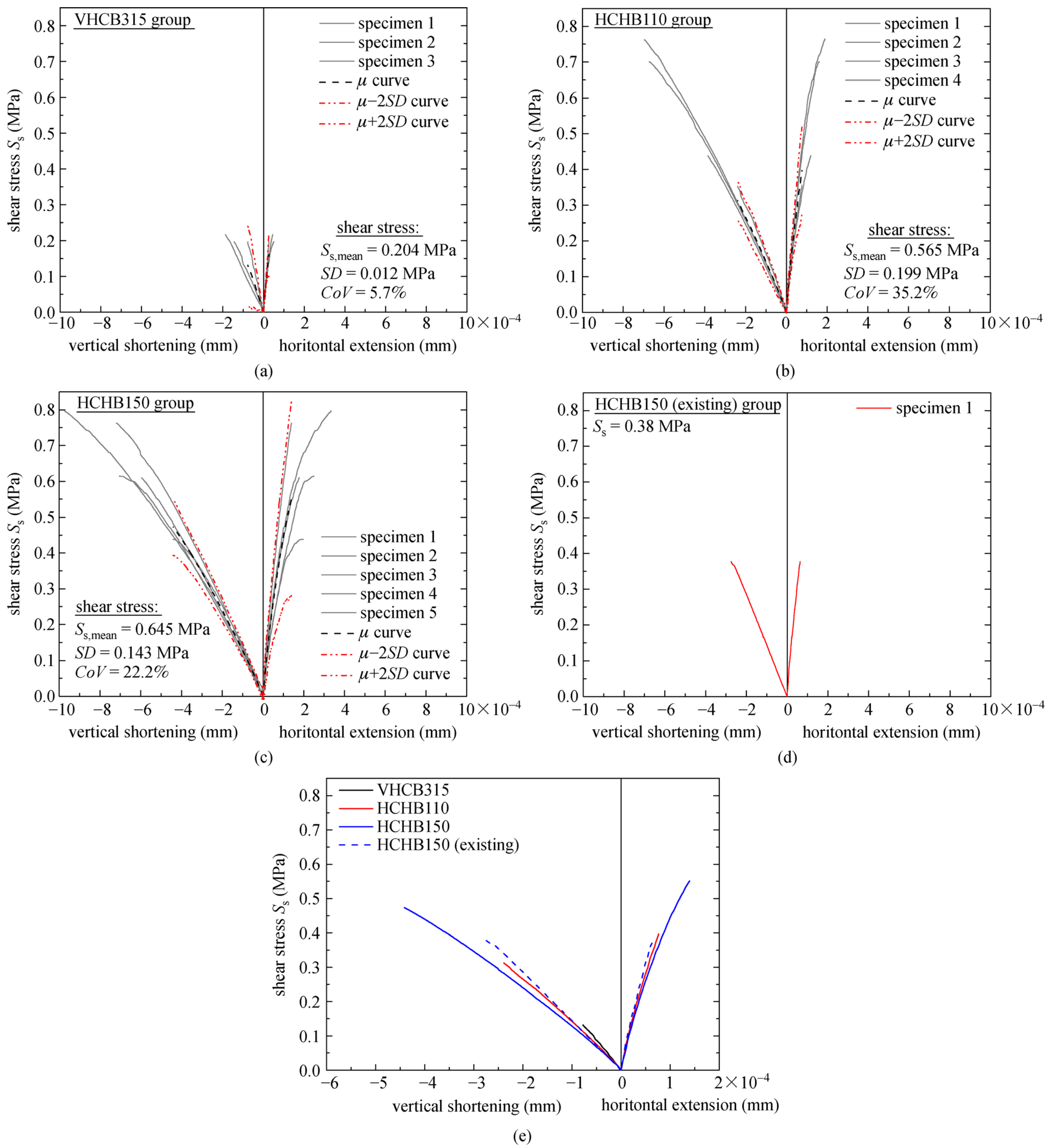

Fig. 11 Diagonal shear tension strength test results: (a) VHCB315; (b) HCHB110; (c) HCHB150; (d) HCHB150 (existent); (e) global comparison.

according to be 600 mm×1000 mm (width × height) for the VHCB315 specimens and 450 mm × 600 mm for the remaining groups (Fig. 16). The standard requires a minimum number of 5 specimens that reach the rupture between the out-of-plane loading horizontal alignments. The standard excludes all tests whose rupture is different than the mentioned before.

No recommendations are provided by the standard for the instrumentation. The standard only demands the load monitoring of the tests. However, in this work, four points distanced from the geometric center (50 mm vertical and 37.5 mm horizontal) were monitored as illustrated in Fig. 16 covering a contour of 100 mm × 75 mm.

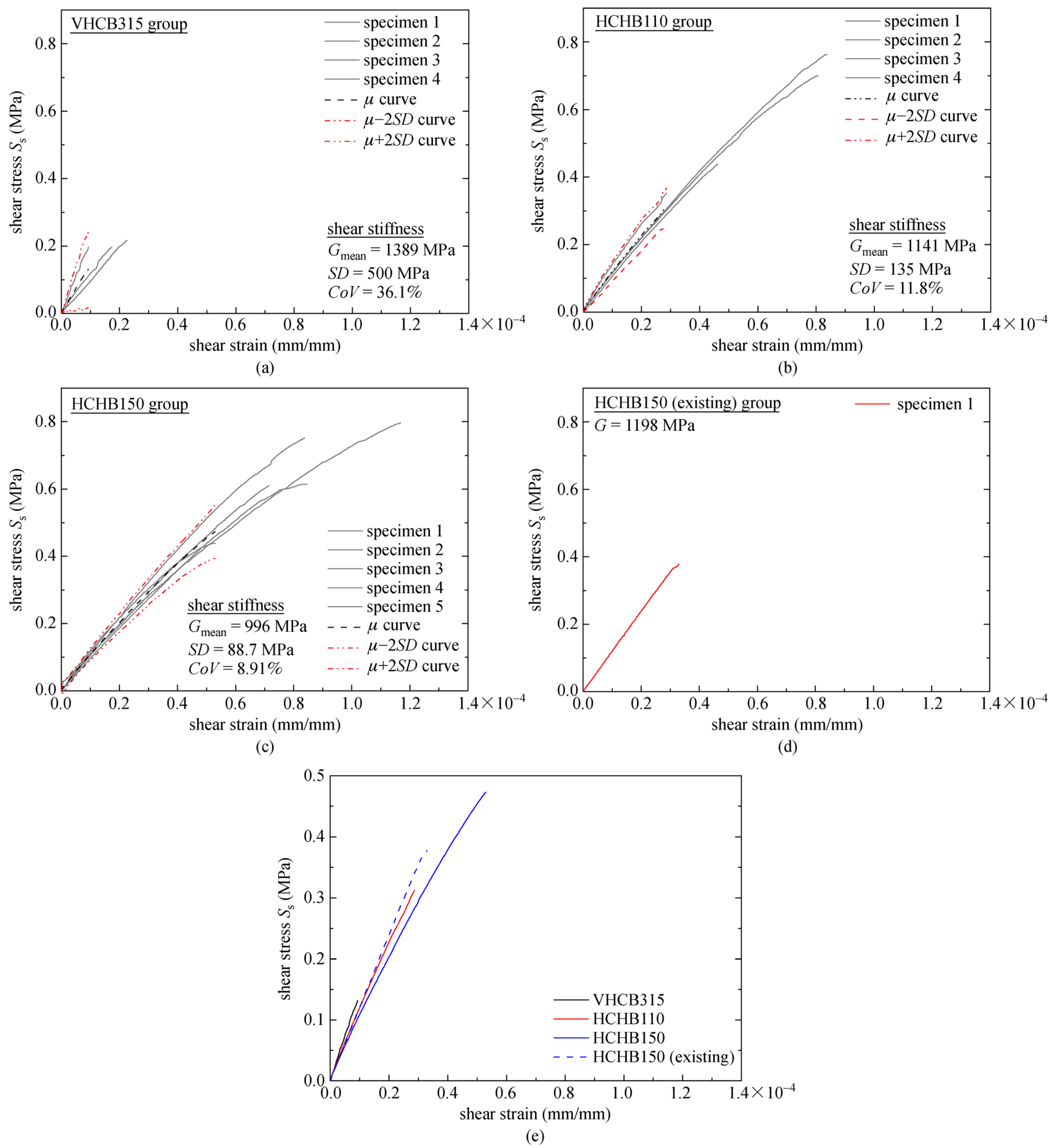

Fig. 12 Diagonal shear strength test results: (a) VHCB315; (b) HCHB110; (c) HCHB150; (d) HCHB150 (existing); (e) global comparison.

Table 8 Rigidity modulus results: statistical parameters

statistical parameter	VHCB315	HCHB110	HCHB150	HCHB150 (existing)
G_{mean} (MPa)	1389	1141	996	1198
SD (MPa)	500.5	135	88.7	N/A
CoV (%)	36.1	11.8	8.91	N/A

Note: N/A: Not applicable.

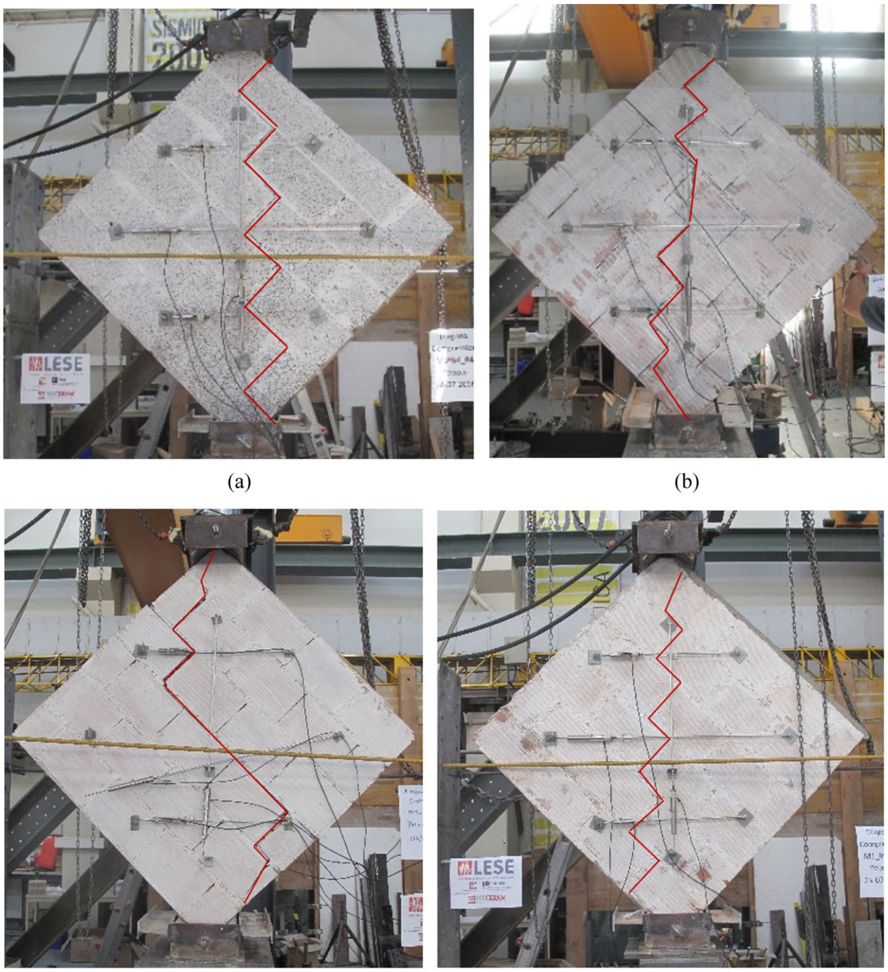

(a) (b) (c) (d)

Fig. 13 Diagonal tensile strength tests: failure modes: (a) VHCB315; (b) HCHB110; (c) HCHB150; (d) HCHB150 (existing).

(a) (b)

Fig. 14 Flexural strength tests parallel to horizontal bed joints: test setup apparatus: (a) lateral view; (b) back view.

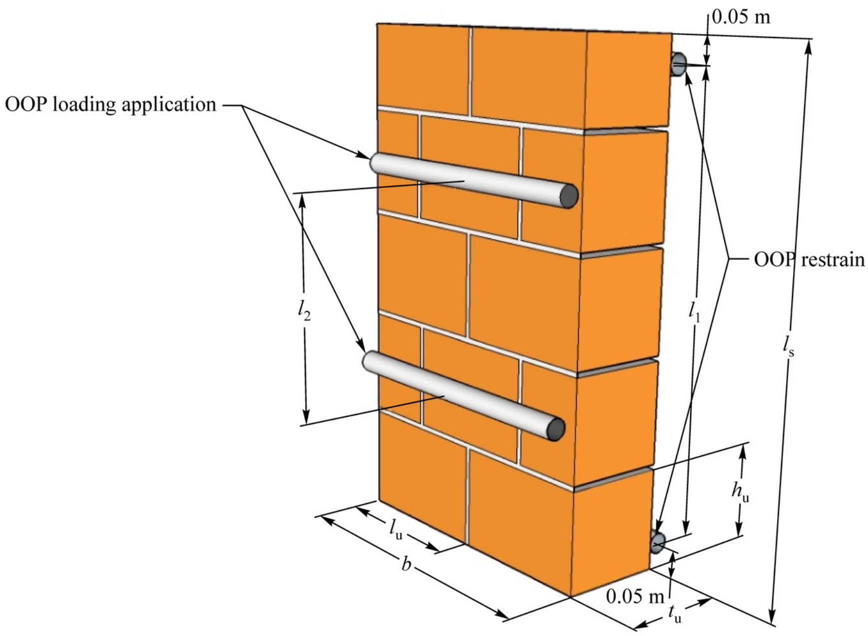

Fig. 15 Flexural strength tests parallel to horizontal bed joints: specimens dimensions according to NP EN1052-2 standard (CEN 1999).

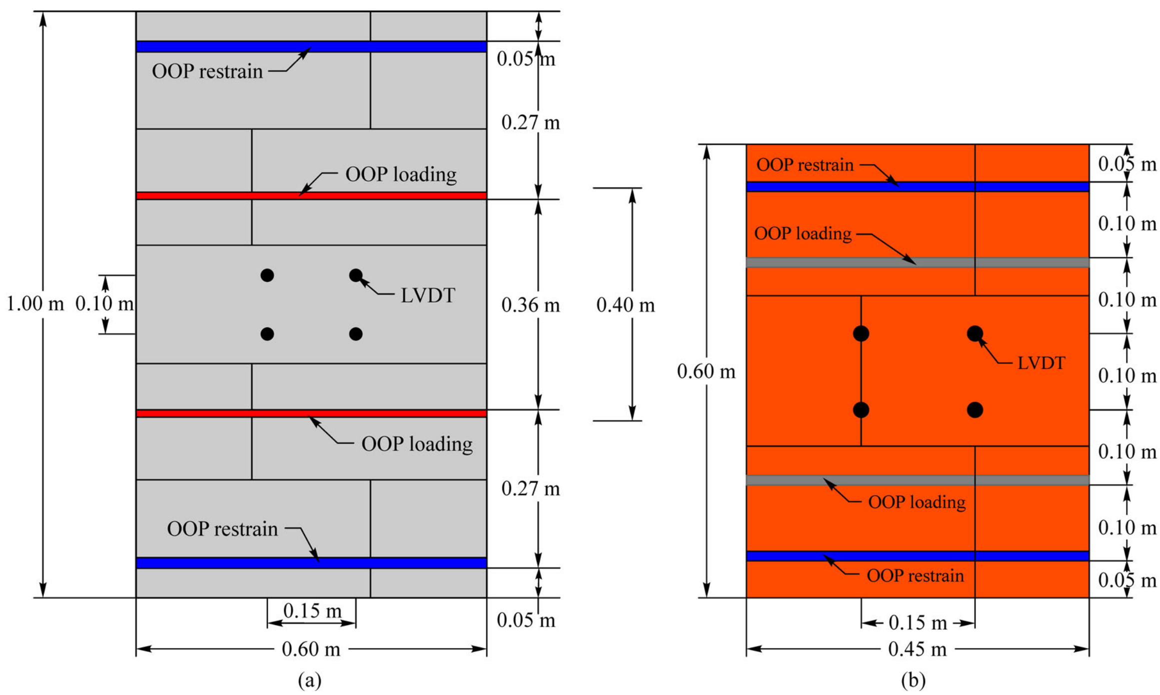

Fig. 16 Flexural strength tests parallel to horizontal bed joints: (a) instrumentation and specimens' dimensions VHCB315; (b) HCB110, HCB150, HCB150P100, HCHB150 (existing), HCHB150P100 (existing).

6.1.2 Force-displacement curves

The flexural strength was determined according to the standard EN 1052-2 (CEN 1999) expression, here expressed by Eq. (10):

$$f_{\mathrm{b,parallel}} = \frac{3 \times f_{i,\max} \times (l_1 - l_2)}{2 \times b \times t_{\mathrm{u}}^2}, \tag{10}$$

where $f_{\mathrm{i,max}}$ is the maximum force applied, l_1 is the distance between restrains, l_2 is the distance between the internal

Table 9 Flexural strength parallel to horizontal bed joints: statistical parameters

statistical parameter	VHCB315	HCHB110	HCHB150	HCHB150P100
$f_{b,mean,paralell}$ (MPa)	0.083	0.117	0.139*	0.218
SD (MPa)	0.014	0.005	0.018	0.038
CoV (%)	14.2	4.26	12.63	17.64
$f_{b,k,paralell}$ (MPa)	0.055	0.078	0.093*	0.145

*Note: Number of tests with rupture according to the standard: 3.

loading application alignments, b is the specimen width and t_u is the specimen thickness. From the testing campaign three specimens HCHB150 did not reached the rupture according to the standard and therefore were excluded from the results. From the force-displacement curves (plotted in Fig. 17), the following observations can be drawn:

1) The highest flexural strength was reached by the group HCHB150P10 (Fig. 17(d)) and lowest one by the VHCB315 (Fig. 17(a)) with a mean value equal to 0.218 and 0.083 MPa, respectively.

2) VHCB315 achieved the lowest flexural strength, about 0.083MPa, 60% of the flexural strength reached by HCHB150 and 71% of the one reached by HCHB110.

3) In Fig. 17(e) it is plotted the response of the existing specimens, with and without plaster, and it is visible again the flexure strength increases of the HCHB150P10 by around 3 times.

4) The highest flexural strength was achieved by the HCHB150P10 group with a mean value of 0.218MPa, meaning that the plaster increased the flexural strength by 57% when compared with the result obtained by the group HCHB150 (note that only 2 tests satisfied the criteria defined by the standard which reduce the amount of data).

5) The variability of the results is lower for the group HCHB110 with a *CoV* of 4.26%, and is higher for the HCHB150P10 with *CoV* equal to 17.64%.

Table 9 presents a summary of the flexural strength statistical parameters collected from the tests in agreement with the EN 1052-2 (CEN 1999).

However, even though the tests were performed according to the standard such in terms of specimens' geometric dimensions or loading protocol and based on the tests observation (type of failure), it must be taken some reservations regarding the results herein expressed. These reservations are related to the fact that these specimens were built with masonry units with certain percentage of voids, which combined with their reduced slenderness ratio could have affected the results and not characterized well the flexural behavior of infill panels made with this type of masonry units. For example, the specimens that were excluded from the battery of tests presented in this work suffered shear failure outside of the region between the OOP loading alignments.

All these factors could have had an important effect in the test results, which could have had resulted in different results than the real expectable ones. Due to this, additional tests must be carried out in long spandrels' specimens (height equal to one-storey height), even without any standard framework. The comparison with these results help to understand if the tests carried out according to minimum geometric dimensions required by the standard EN 1052-2 (CEN 1999) are representative or not of the real expectable behavior and capacity of panels made with these masonry units.

6.1.3 Damages observed

From the observation of the specimens' rupture, all of them were characterized by the detachment between the masonry unit and the horizontal bed joint in the existing joints along distance between the internal loading application alignments specimens. The specimens which rupture were not according to the standard, were due to shear failure in the alignment of the load application. Figure 18 presents the most representative failure modes obtained observed of each group of specimens.

6.2 Perpendicular to the horizontal bed joints

6.2.1 Introduction

Complementarily, flexural strength tests perpendicular to the horizontal bed joints were carried out according to the standard EN1052-2 (CEN 1999). The test setup adopted was similar to that one described in the previous section, with the main differences relative the linear out-of-plane loading that is applied in the vertical direction as well as the restrains supports (Fig. 19).

The standard NP EN1052-2 standard (CEN 1999) requires the following specifications for the definition of the specimens' dimensions (Fig. 20), namely:

For masonry units with height larger than 250 mm:

1) Specimen width must have to be larger than 1000 mm.

2) At least one vertical joint should exist along the distance l_2.

For masonry units with height equal or lower than 250 mm:

1) Specimen width must have to respect these conditions: $b \geqslant 240$ mm and $b \geqslant 3h_u$.

2) At least one vertical and one horizontal joint should

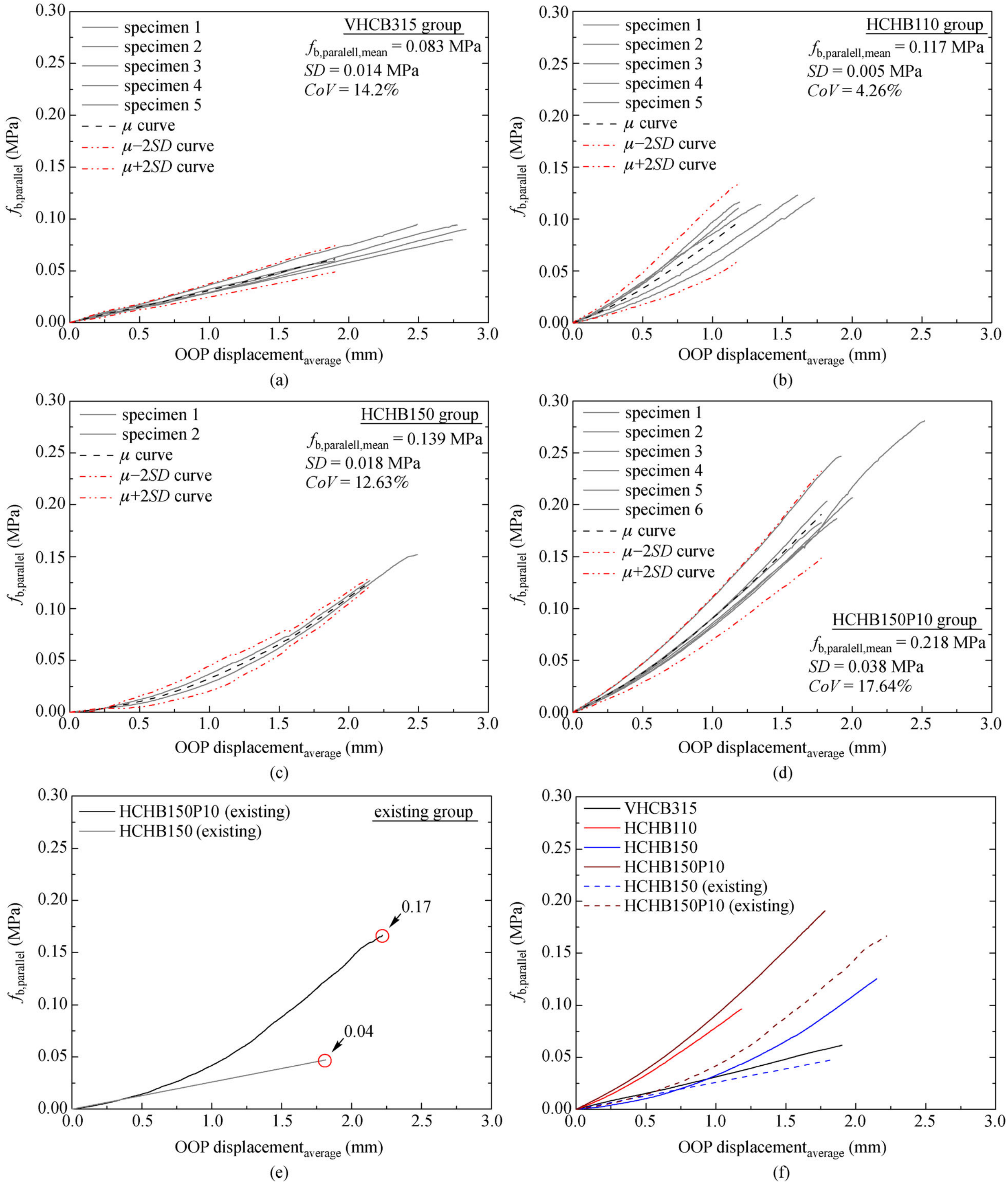

Fig. 17 Flexural strength tests parallel to horizontal bed joints: Flexural strength vs OOP displacement: (a) VHCB315; (b) HCB110; (c) HCB150; (d) HCHB150P10; (e) HCB150 (existing) and HCHB150P10 (existing); (f) global results.

exist along the distance l_2.

The specimens' geometric dimensions were defined according to the standard requirements, namely: 1200 mm × 800 mm (width × height) for the VHCB315 group with the linear load applied at a distance of 370 mm from each other and the restrains at 1100 mm apart (Fig. 21(a)). The remaining groups' geometric dimensions are 600 mm × 600 mm (width × height) with the load application distanced from 300 mm from each other and the restrains 500 mm, respectively (Fig. 21(b)).

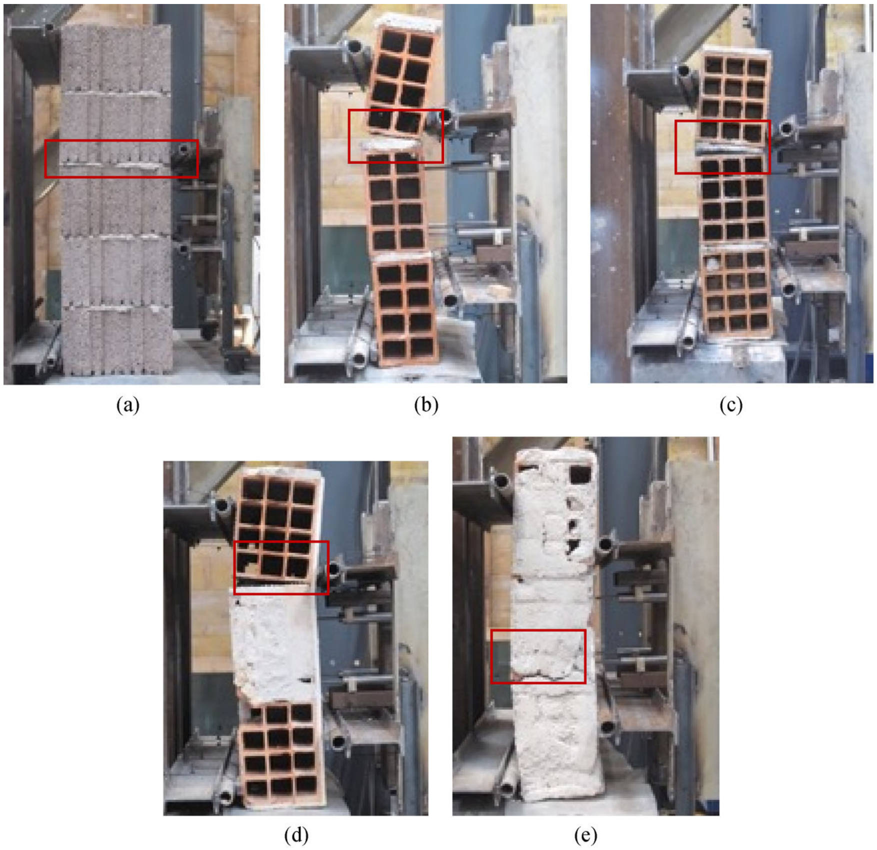

Fig. 18 Flexural strength tests parallel to horizontal bed joints failure modes: (a) VHCB315; (b) HCHB110; (c) HCHB150; (d) HCHB150P10 (existing); (e) HCHB150 (existent).

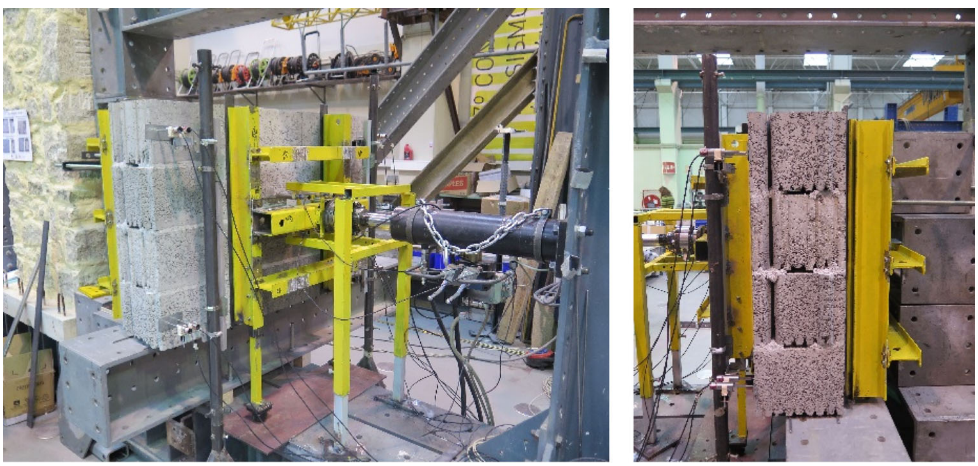

(a) (b)

Fig. 19 Flexural strength tests perpendicular to horizontal bed joints: test setup apparatus: (a) lateral view; (b) back view.

The instrumentation adopted for these tests was the same described in the flexural tests parallel to the horizontal bed joints and is illustrated in Figs. 21(a) and 21(b). As mentioned for the flexure tests parallel to the bed joints, the standard EN 1052-2 (CEN 1999) only considers specimens which rupture occurred between the linear out-of-plane loading alignments.

6.2.2 Force-displacement curves

The flexural strength was estimated according to Eq. (10). One specimen from the HCHB110 group did not reach the

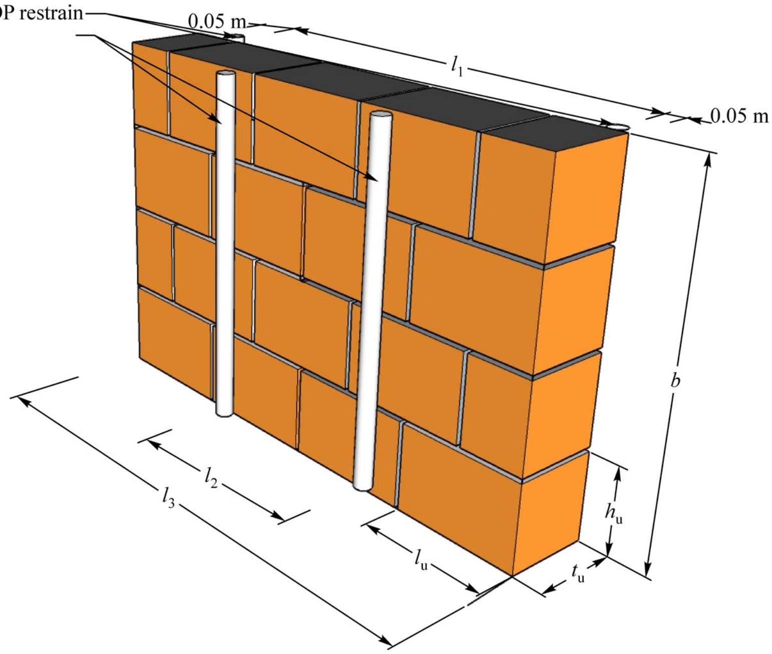

Fig. 20 Flexural strength tests perpendicular to horizontal bed joints: specimens dimensions according to NP EN1052-2 standard (CEN 1999).

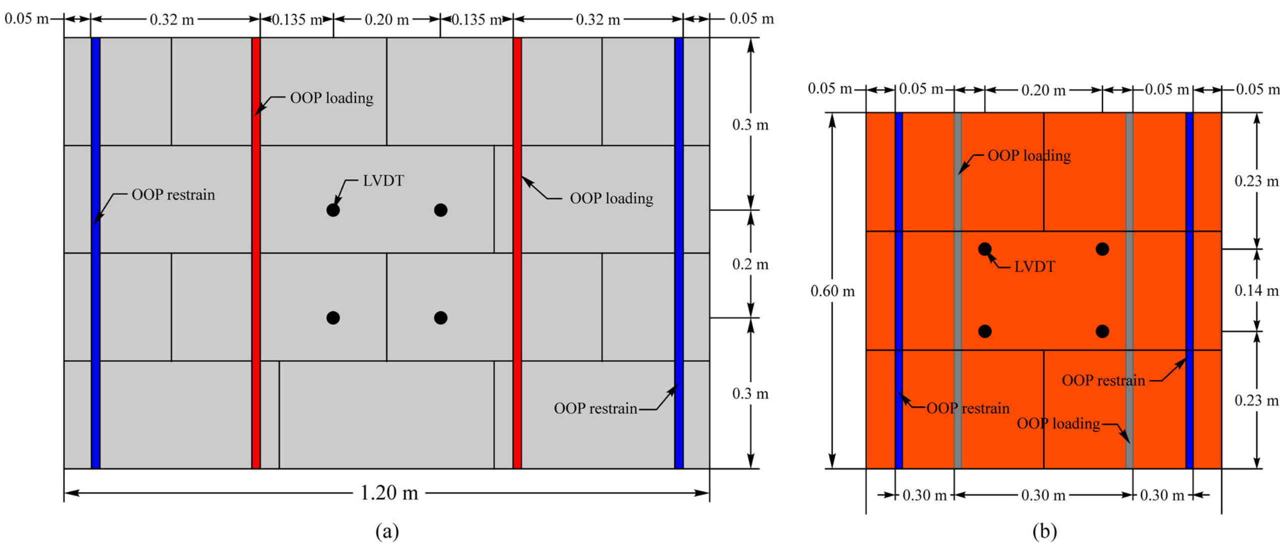

Fig. 21 Flexural strength tests perpendicular to horizontal bed joints instrumentation and specimens' geometric dimensions: (a) VHCB315; (b) HCB110; HCB150; HCB150P10; HCHB150 (existing).

rupture according to the standard and was not considered for the analysis. From the force-displacement curves (Fig. 22), the following observations can be drawn:

1) VHCB315 reached the lowest flexural strength of the testing campaign, namely 39% lower than HCHB110 and 49% than HCHB150.

2) HCHB150 specimens achieved the highest flexural strength with a mean value of 0.322 MPa, which is 6% higher than the results obtained by the HCHB150P10 group. The reason behind this difference can be attributed to the results variability.

3) Lower difference is observed when it is compared the HCHB110 and the HCHB150 results, with the first ones reaching an average value of 0.271 MPa, 11% less than the last one.

4) The results of the HCHB150 (existing) group are 19% lower than these reached by the as-built group, assuming the *CoV* of 25.1% obtained by the HCHB150

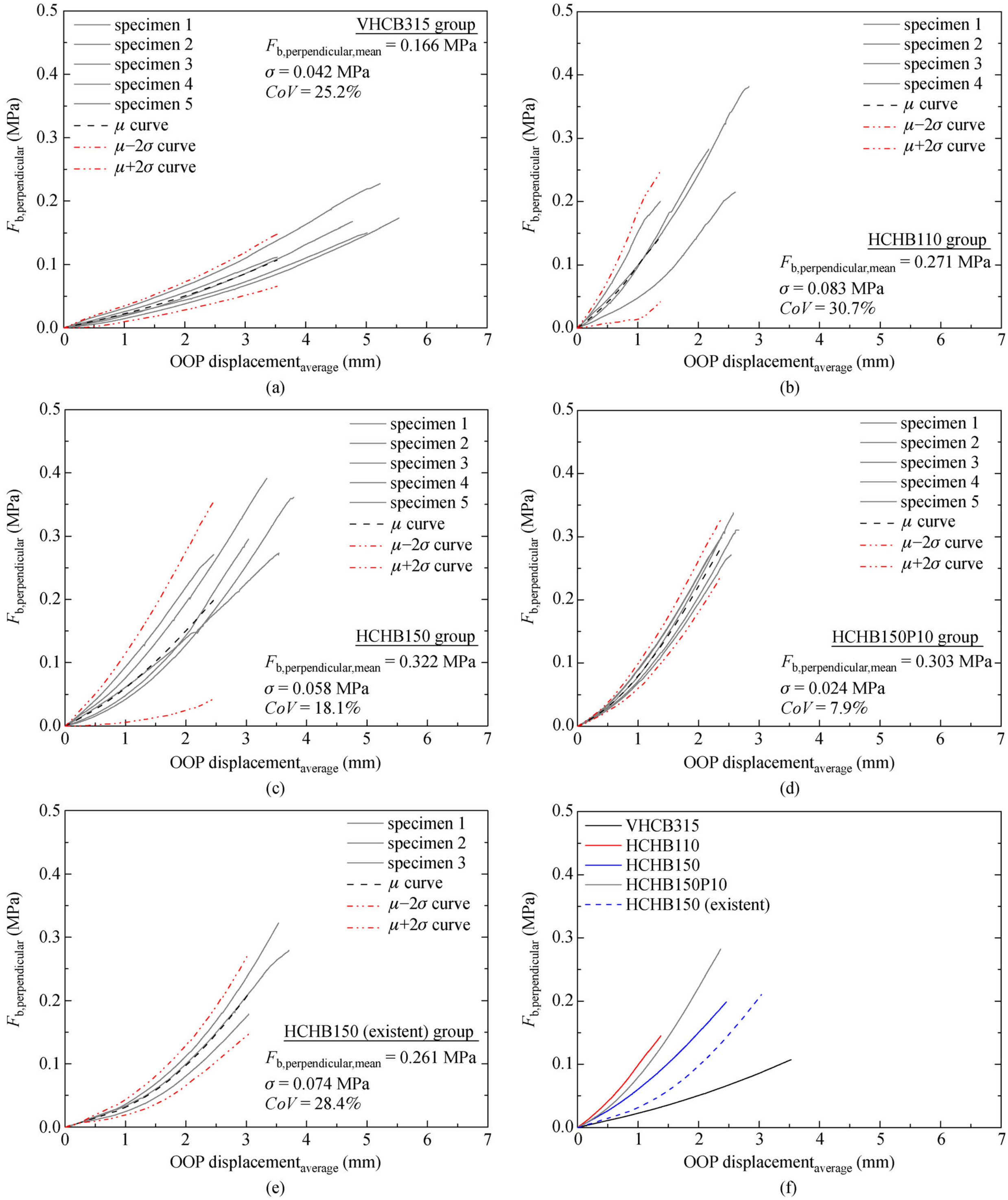

Fig. 22 Flexural strength tests perpendicular to horizontal bed joints stress vs OOP displacement: (a) VHCB315; (b) HCHB110; (c) HCHB150; (d) HCHB150P10; (e) global results.

this value is reasonable.

5) The group with lower variability of the results is the HCHB150P10 with a *CoV* equal to 7.9%. The largest difference was achieved by the HCHB110 group.

Table 10 provides a summary of the flexural strength statistical parameters collected from the tests in agreement with the EN 1052-2.

6.2.3 Damage observed

The typical failures occurred throughout the flexural tests were characterized by vertical crack of the specimens in

Table 10 Flexural strength perpendicular to horizontal bed joints: summary of test results

statistical parameter	VHCB31.5	HCHB110	HCHB150	HCHB150P100	HCHB150 (existent)
$f_{b,perpendicular,mean}$ (MPa)	0.166	0.271	0.322	0.303	0.261
SD (MPa)	0.042	0.083	0.058	0.024	0.074
CoV (%)	25.2	30.3	18.1	7.9	28.4
$f_{b,k,perpendicular}$ (MPa)	0.111	0.181	0.215	0.202	N/A

their middle alignment of the specimen. Total rupture of the central masonry units was observed. Examples of the specimens' failures are presented in Fig. 23.

7 Discussion of results from experimental testing

Table 11 summarizes the main properties obtained within this experimental campaign. From the compressive strength tests, the following conclusions can be highlighted higher mean compressive strength and elastic modulus was obtained for the VHCB315 group, and the lower ones were obtained for the HCHB110 group. Concerning the elastic modulus of the specimens made with concrete blocks is at least 65% higher than these made with HCHB. Looking for the global results of the VHCB315 panels, it is possible to observe that achieved the lowest diagonal tensile strength, shear modulus, and flexural strength, but higher compressive strength. This interesting result is due to the construction methodology described in Section 2, where the absence of full filled mortar joints (horizontal and vertical) played an important role in the specimens' experimental response.

From the diagonal tensile strength tests the following conclusions can be highlighted:

1) Higher mean shear tensile strength and transverse stiffness were obtained for the HCHB150 group while the lower ones were achieved in the VHCB315 group.

2) The strength obtained by the HCHB150 is 14% higher than that obtained by HCHB110 group.

3) The transverse stiffness modulus obtained by the VHCB315 group is 43% of the compressive elastic modulus which results in a Poisson coefficient approximately equal to 0.17. Regarding the HCHB groups, it was obtained a transverse stiffness modulus of 62% and 51% of the compressive elastic modulus for the specimens with 110 and 150 mm thickness, respectively.

4) Fragile behavior was observed in the panels made with clay bricks with horizontal perforation, without propagation of cracks. Furthermore, some sliding failures were observed within the tests.

5) Development of vertical cracks occurred during the increase of the vertical compressive forces in the specimens made by concrete blocks. No fragile behavior was observed.

From the flexural strength tests the following conclusions can be highlighted:

1) VHCB315 specimens achieved lower strength results when compared with the HCHB110 and HCHB150 groups;

2) higher variability of the test results for the flexural strength tests perpendicular to the horizontal bed joints;

3) the plaster increases the flexural strength capacity of the specimens made with clay bricks with horizontal perforation.

8 Conclusions

An experimental campaign was carried out aiming at characterizing the mechanical properties of three types of infill masonry walls made with different types of masonry units: VHCB315, HCHB150, and HCHB110. A total number of 80 tests were carried out such in infill panels to achieve the corresponding mechanical properties, such in terms of compressive strength, diagonal tensile strength and flexural strength. Additionally, it was performed a comparison between results of as-built specimens and results from specimens that were collected from existing walls (built in laboratory from full-scale tests) to assess and discuss possible differences between them. From the experimental tests, it was observed fragile behavior was observed in the panels made with clay bricks with horizontal perforation, without propagation of cracks. The collapse of parts of the bricks with the increase of the vertical compressive force, increased the instability of the panel and resulted in fragile collapses of the specimens. The development of vertical cracks was found throughout the increase of the vertical compressive strength in the specimens made by concrete blocks. As observed in the compressive strength tests, fragile behavior was observed in the panels made with clay bricks with horizontal perforation, without propagation of cracks. Furthermore, some sliding failures were observed within the tests.

The compressive strength of the panels made with VHCB315 reached the highest compressive strength about 3 times higher than the lowest one obtained by the HCHB110. The compressive strength of the HCHB150 panels is 40% higher than the HCHB110. The existing panels seems to have a compressive strength 10% higher than the as-built ones.

Fig. 23 Flexural strength tests parallel to horizontal bed joints failure modes: (a) VHCB315; (b) HCHB110; (c) HCHB150; (d) HCHB150P10 (existing); (e) HCHB150 (existing).

Table 11 Summary of mechanical properties obtained from the experimental campaign

mechanical properties	VHCB315	HCHB110	HCHB150	HCHB150P10
$f_{c,mean}$ (MPa)	1.82	0.66	0.806	N/A
E_{mean} (MPa)	3251	1837	1975	N/A
S_s (MPa)	0.204	0.565	0.645	N/A
G (MPa)	1389	1141	996	N/A
$f_{b,parallel,mean}$ (MPa)	0.083	0.117	0.139	0.218
$f_{b,perpendicular,mean}$ (MPa)	0.166	0.271	0.322	0.303

Concerning the diagonal tensile strength, the panels HCHB150 achieved the highest result about 3 times higher than the lowest one which was obtained by the specimens VHCB315. Finally, the highest flexural strength was reached by the panels made with HCHB150P10, which revealed the important effect of the plaster which increase the flexural capacity of the panels about 57% when compared with the specimens without plaster. The mortar adhesion properties play an important role in the flexural capacity of the specimens parallel to the horizontal bed joints.

Notation

$f_{c,m}$	mortar compressive strength
$f_{t,m}$	mortar flexural strength
f_c	masonry infill panels compressive strength
$f_{c,mean}$	masonry infill panels mean compressive strength
$f_{c,k}$	masonry infill panels characteristic compressive strength
E_{mean}	mean masonry infill walls elasticity modulus
μ	average value
σ	standard deviation
CoV	coefficient of Variation
R_w	masonry unit sound insulation resistance
R_t	masonry unit thermal resistance
$f_{c,unit}$	masonry unit compressive strength perpendicular to the holes
S_s	masonry infill panels shear stress
$S_{s,mean}$	masonry infill panels mean shear stress
γ	mhear straining
G_{mean}	mean masonry infill panels rigidity modulus
$f_{b,parallel}$	masonry infill panels flexural strength parallel to the horizontal bed joints
$f_{b,parallel,mean}$	mean masonry infill panels flexural strength parallel to the horizontal bed joints
$f_{b,parallel,k}$	characteristic masonry infill panels flexural strength parallel to the horizontal bed joints
$f_{b,perpendicular}$	masonry infill panels flexural strength perpendicular to the horizontal bed joints
$f_{b,perpendicular,mean}$	mean masonry infill panels flexural strength perpendicular to the horizontal bed joints
$f_{b,perpendicular,k}$	characteristic masonry infill panels flexural strength perpendicular to the horizontal bed joints

Acknowledgements The authors would like to acknowledge the support financially support by: Project POCI-01-0145-FEDER-007457-CONSTRUCT-Institute of R&D in Structures and Construction funded by FEDER funds through COMPETE2020—Programa Operacional Competitividade e Internacionalização (POCI) and by national funds through FCT-Fundacão para a Ciencia e a Tecnologia, namely through the research project P0CI-01-0145-FEDER-016898-ASPASSI-Safety Evaluation and Retrofitting of Infill masonry enclosure Walls for Seismic demands. The authors would like to acknowledge the technicians of the Laboratory of Earthquake and Structural Engineering (LESE), Mr. Valdemar Luis, Mr. Guilherme Nogueira and Mr. Nuno Pinto for their support in the experimental activity reported in this paper. Finally, the authors want to acknowledge to Artebel and Preceram for the provision of all the concrete blocks and bricks used in the experimental tests.

References

1. Furtado A, Rodrigues H, Arêde A, Varum H. Out-of-plane behavior of masonry infilled RC frames based on the experimental tests available: A systematic review. Construction and Building Materials, 2018, 168: 831–848
2. Di Domenico M, Ricci P, Verderame G M. Experimental assessment of the influence of boundary conditions on the out-of-plane response of unreinforced masonry infill walls. Journal of Earthquake Engineering, 2018 (in press)
3. Kadysiewski S, Mosalam K M. Modeling of unreinforced masonry infill walls considering in-plane and out-of-plane interaction. In: The 11th Canadian Masonry Symposium. Toronto: Pacific Earthquake Engineering Research Center, 2009
4. Furtado A, Rodrigues H, Arêde A, Varum H. Simplified macro-model for infill masonry walls considering the out-of-plane behaviour. Earthquake Engineering & Structural Dynamics, 2016, 45(4): 507–524
5. Asteris P G, Cavaleri L, Di Trapani F, Tsaris A K. Numerical modelling of out-of-plane response of infilled frames: State of the art and future challenges for the equivalent strut macromodels. Engineering Structures, 2017, 132: 110–122
6. Di Trapani F, Shing P B, Cavaleri L. Macroelement model for in-plane and out-of-plane responses of masonry infills in frame structures. Journal of Structural Engineering, 2018, 144(2): 04017198
7. Singhal V, Rai D C. Suitability of half-scale burnt clay bricks for shake table tests on masonry walls. Journal of Materials in Civil Engineering, 2014, 26(4): 644–657
8. Ferretti D, Michelini E, Rosati G. Mechanical characterization of autoclaved aerated concrete masonry subjected to in-plane loading: Experimental investigation and FE modeling. Construction and Building Materials, 2015, 98: 353–365
9. Cavaleri L, Papia M, Macaluso G, Di Trapani F, Colajanni P. Definition of diagonal Poisson's ratio and elastic modulus for infill masonry walls. Materials and Structures, 2014, 47(1): 239–262
10. Knox C L, Dizhur D, Ingham J M. Experimental study on scale effects in clay brick masonry prisms and wall panels investigating compression and shear related properties. Construction and Building Materials, 2018, 163: 706–713
11. CEN. EN 1052-1: Methods of Test for Masonry, Part 1: Determination of Compressive Strength. London: British Standards Institution, 1998
12. ASTM. E 519-02. Standard Test Method for Diagonal Tension (Shear) in Masonry Assemblages. West Conshohcken: American Society for Testing and Materials, 2002
13. RILEM. RILEM TC 76-LUM. Diagonal Tensile Strength of Small Walls Specimens. RILEM Publications SARL, 1994
14. CEN. EN 1052-2: Methods of Test for Masonry, Determination of

Flexural Strength. London: British Standards Institution, 1999
15. CEN. EN 1015-11: Methods of Test for Mortar for Masonry, Part 11: Determination of Flexural and Compressive Strength of Hardened Mortar. London: British Standards Institution, 2004
16. Pereira P, Pereira M, Ferreira J, Lourenço P. Behavior of masonry infill panels in RC frames subjected to in plane and out of plane loads. In: The 7th Conference on Analytical Models and New Concepts in Concrete and Masonry Structure Cracow. Poland, 2012
17. Sahlin S. Structural Masonry. New Jersey: Prentice-Hall Inc., 1971
18. Sinha B P, Pedreschi R. Compressive strength and some elastic properties of brickwork. International Journal of Masonry Construction, 1983, 3(1): 19–27
19. Bartolomé S A, Quiun D, Barr K, Pineda C. Seismic Reinforcement of Confined Masonry Walls made with Hollow Bricks using Wire Meshes. In: The 15th World Conference on Earthquake Engineering. Lisbon, 2012
20. Hendry A W. Structural Masonry. London: Macmillan Education Ltd., 1990
21. Paulay T, Priestley M J N. Seismic design of RC and masonry buildings. New York: Wiley Interscience, 1992
22. European Committee for Standardisation. Eurocode 6: Part 1-1–General Rules for Buildings–Rules for Reinforced and Unreinforced Masonry. Brussels: European Committee for Standardisation, 2005